Hsu, L. T. (2017, October). GNSS multipath detection using a machine learning approach. In Intelligent Transportation Systems (ITSC), 2017 IEEE 20th International Conference on (pp. 1-6). IEEE.
https://doi.org/10.1109/ITSC.2017.8317700

GNSS Mulitpath Detection Using a Machine Learning Approach

Li-Ta Hsu
Interdisciplinary Division of Aeronautical and Aviation Engineering
The Hong Kong Polytechnic University
The Hong Kong Polytechnic University, Hung Hom, Kowloon, Hong Kong
lt.hsu@polyu.edu.hk

***Abstract*— Insufficient localization accuracy of global navigation satellite system (GNSS) receivers is one of the challenges to implement advanced intelligent transportation system in highly urbanized areas. Multipath and non-line-of-sight (NLOS) effects strongly deteriorate GNSS positioning performance. This paper aims to train a classifier by supervised machine learning to separate the type of GNSS pseudorange measurement into three categories, clean, multipath and NLOS. Several features obtained or calculated from the GNSS raw data are evaluated. This paper also proposes a new feature to indicate the consistency between measurements of pseudorange and Doppler shift. According to the experiment result, about 75% of classification accuracy can be achieved using a support vector machine (SVM) classifier trained by the proposed feature and received signal strength.**

Keywords—Global Positioning System, Multipath, NLOS, Support Vector Machine, Urban Area, Machine Learning

I. INTRODUCTION

Smart mobility is one of the six major components of the smart city development. Global navigation satellite system (GNSS) localization is essential to the smart mobility for different applications, including pedestrian [1] and vehicle navigation [2], fleet management [3], road traffic monitoring and analysis [4], road user charging (RUC) [5], irregular driving detection [6] etc. This paper focuses on the vehicle and pedestrian localization for the autonomous driving application.

As the maturity and popularity of the pedestrian-to-vehicle (P2V) and vehicle-to-vehicle (V2V) communications [7, 8], the collision avoidance between pedestrian and autonomous vehicles could be achieved in the coming future. One of the current bottlenecks of the intelligent collision avoidance is the localization accuracy of pedestrian and vehicle. Generally speaking, GNSS receiver is the most common device/chip to provide absolute positioning information to the carriers. GNSS positioning performance is currently very satisfactory in the area with good satellite observing condition such as highway, express way, sub-urban and rural areas. Its positioning performance in urban area is a different story. The notorious multipath effect in dense building environment is dramatically reducing the GNSS localization accuracy. The multipath effect is sourced from the reflection and diffraction of satellite signal by the tall buildings and skyscrapers. It could easily deteriorate the GNSS accuracy to several tens of meters [9]. Comparing with the multipath effects, a more devastating phenomenon is non-line-of-sight (NLOS) reception. The difference between multipath and NLOS can be demonstrated as Fig.1. Multipath contains both the line-of-sight (LOS) and reflected signals while NLOS contains only the latter one.

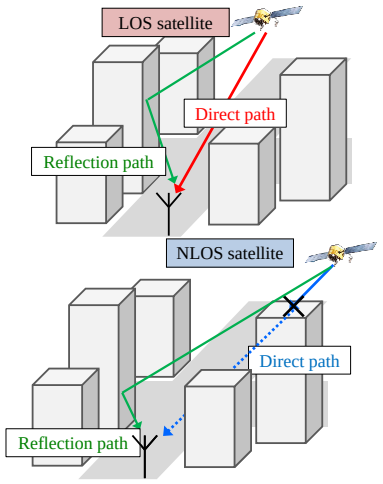

Fig. 1. The multipath and NLOS effects in an urban canyon. (a) Multipath effect, (b) NLOS propagation [1].

The multipath effect could be roughly mitigated using sophisticated receiver correlator designs [10]. The principle of the correlator design is comparing the early, prompt and late channels in code tracking loop [11]. In the other words, it compares the direct signal with reflected one. Unfortunately, this design does not mitigate the NLOS effect at all because the NLOS contains only the reflected signal. Thus, the research focused on detection and mitigation of NLOS is increasing. The NLOS detection methods can be categorized into antenna [12], advanced receiver algorithm [13, 14], sensors integration [15], 3D building model and machine learning. The detail of the latter two methods will be discussed in the next section.

This paper aims to develop a LOS, multipath, NLOS classifier based on machine learning algorithm. The pivot of successful machine learning is to identify the significant features. Thus, several variables obtained or calculated from the GNSS raw data is evaluated. The raw data denotes the pseudorange, carrier to noise ratio, Doppler shift frequency and carrier phase measurements which can be archived as RINEX format [16]. According to the recent announcement of Google,

all the new smartphone with Android Nougat OS can support the output of the above listed measurements [17]. Namely, an assumption can be made that the potential features extracting from the GNSS raw data is able to be obtained from most of the new GNSS devices. The novelty of this paper is to not only classifying clean and biased measurements but also further distinguish multipath and NLOS from the biased measurements.

II. RELATED RESEARCH

A. GNSS with 3D buildings

Due to the rise of smart cities, the 3D city models are rapidly developed and became widely available. Recent research stream of dealing with multipath and NLOS is to utilize 3D mapping and is called as 3D mapping aided (3DMA) positioning methods. One of the most well-known 3DMA method is shadow matching [18, 19]. It takes advantage of making building boundary to predict satellite visibility from the 3D city model. Researchers are also focused on improved GNSS positioning accuracy using enhanced 3D digital map [20-22]. Instead of mitigating or excluding NLOS effect, in the past few years, the potential of using NLOS signal in constructive senses is proposed [1, 23, 24]. Researchers propose to combine ray-tracing simulation with hypothesis-based positioning method to further improve the positioning accuracy. These range-based 3DMA uses a ray-tracing technique to estimate the reflection route of NLOS signal. The route is then used to correct the NLOS delay from the biased pseudorange measurement and finally it further improved positioning accuracy to about 5 meters for pedestrian applications [25]. However, the range-based method cannot be easily adapted to low-cost receiver due to the heavy computational load caused by ray-tracing and the inaccessibility to 3D building models in real-time. In this paper, the ray-tracing simulation and 3D building model will be used in the offline stage to label the measurement into LOS, multipath and NLOS.

B. GNSS using machine learning

The discussion of GNSS using machine learning to facilitate its localization starts from 2013. The first idea is to classify the location accuracy into three accuracy bands based on the combination of number of satellite, dilution of precision (DOP), received signal strength and receiver speed [26]. A Wilcoxon-norm-regressor based on pseudorange residual is proposed to detect biased pseudorange measurement [27]. Researchers also select elevation and azimuth angles as the key features in their machine learning to mitigate multipath effect for static applications [28]. Variable from the correlators in the receiver signal processing stages are extracted to classify the six typical scenarios of GNSS receiver [29]. In 2016, the idea of machine learning to detect NLOS is also implemented in Nav2Nav application, which is well-known as the vehicle cooperative navigation [30]. A decision tree approach is used to classify LOS and NLOS based on receiver signal strength and elevation angle [31]. In this paper, we investigate several features used in the related work. In addition, the measurement of Doppler shift is also used as key feature in the proposed classifier trained by support vector machine (SVM).

III. GNSS DATA COLLECTION AND LABELLING

In order to record a large amount of multipath and NLOS data, we set up a static experiment in a dense building area in Hung Hom, HK. Fig. 2 demonstrates the environment that the data was collected. The antenna is attached with a stick and put outside of the window for long time data collection. Commercial GNSS receiver, u-blox M8, is deployed to collect multipath and NLOS data. 24 hours of the biased GNSS raw measurement are collected. In this dataset, almost all the measurements are affected by the building in the vicinity. In the other words, this urban dataset only contains multipath and NLOS measurements.

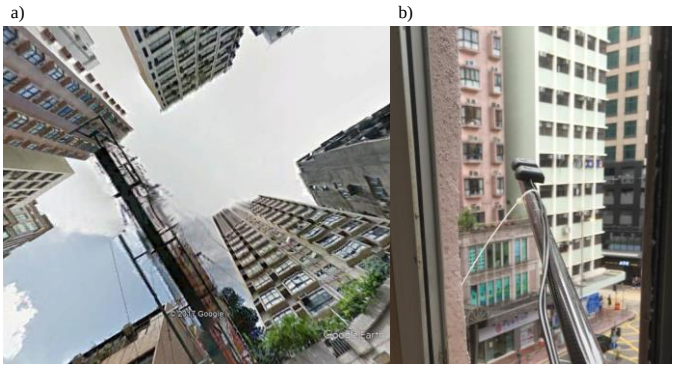

Fig. 2. a) denotes the environment of the multipath and NLOS data was collected and b) indicates the installment of the patch antenna.

Labelling multipath and NLOS signals from the urban data is challenging because of the implicit signal transmission. Our idea is to implement the ray-tracing simulation to identify the signal transmitting types. The principle of ray-tracing in GNSS is to use the known satellite, reflector and receiver geometry to trace the direct and reflecting path. The detail of the ray-tracing in the simulation of GNSS multipath can be found in [32]. The satellite position can be estimated by the broadcast ephemeris. The reflector is searched from the 3D building models. We manually construct basic 3D building models of Hung Hom area by referencing the 3D model in Google Earth as Fig. 3.

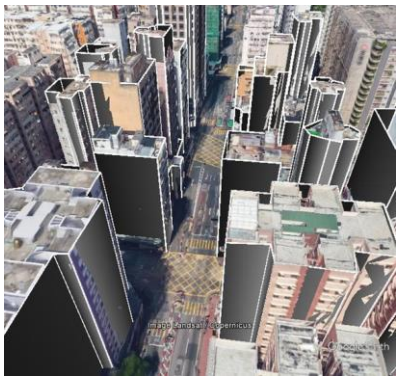

Fig. 3. Constructed 3D building models in Kowloon, HK (courtesy of Google Earth).

In the labelling stage, the receiver is set statically in the experiment so that the ground truth of receiver position can be easily determined. The ground truth is given by the topographic map brought from land department of HK government. The resolution of the map is 20 centimeter (cm). Each point is given

with accurate 2D coordinate. The height is given by the topography height obtained from Google plus the height of equipment. Once the positions of satellite, reflector and receiver are known, the ray-tracing simulation can be performed.

Fig.4 shows the skyplot of the urban dataset. This skyplot is generated using ray-tracing and 3D building model. The grey area in Fig.4 indicates the direct transmission is blocked according to the building models. It is clear that many NLOS propagations are received in the biased dataset.

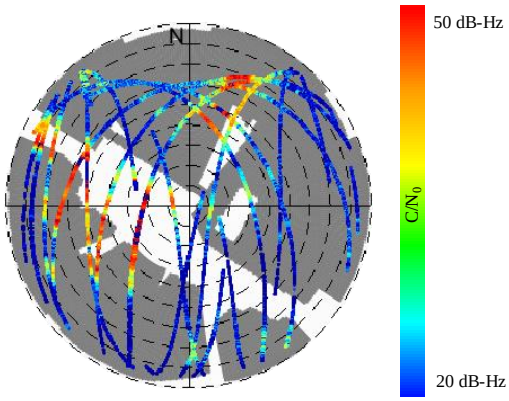

Fig. 4. Skyplots with surrounding building information of data collected in HK. The color of satellite trajectory denotes received signal strength, the redder the color is, the higher of the signal strength received.

The algorithm of NLOS identification is described as following.

Algorithm 1: NLOS and multipath separation using ray-tracing simulation and building model	
STEP1:	Prepare a line segment connecting the receiver and the satellite of the measurement (*i*).
STEP2:	Initialize signal type of measurement (*i*) as Multipath
STEP3:	**for all** the building model $\mathbf{B}^j$ **do**
STEP3:	**for all** planes (walls) $\boldsymbol{w}_k^j$ of a building **do**
STEP4:	**if the** intersection between the line segment and plane w_k^j exists **then**
STEP5:	the measurement identified as NLOS
	break
	end if
STEP6:	**end for** planes
STEP7:	**end for** buildings

Regarding to LOS (clean) GNSS data, HK land department establishes a GNSS network called *SatRef* to provide differential correction for HK users. We adopt the archived RINEX data of the SatRef station as the LOS data because the reference station is located in place with great observing condition. 24 hours of clean data is also used in training the classifier.

Observing Fig.4, we can discover that the received signal strength of NLOS signal at lower elevation angle is also lower. Namely, it implies the NLOS can be identified using the combination of different variables. Next section discusses the variables that can be used to classify the measurement types.

IV. Features to Classify LOS/NLOS/Multipathh Measurement

LOS signal contains only direct signal from the satellite to receiver. NLOS reception denotes only the signal reflection received by the receiver. Multipath contains both direct and reflecting signal. Based on the nature of their differences, the following variables could be hints to separate the measurements.

Received signal strength, RSS: Received signal strength is usually represented by carrier to noise ratio (C/N_0). Due to the theory of signal propagation, additional travelling and reflection will increase the signal propagation loss. Thus, it is one of the most popular variable to be used to mitigate multipath effects. The RSS data can be easily obtained from NMEA and RINEX data format.

Change rate of received signal strength, ΔRSS: Due to the principle of receiver tracking loop, the received signal strength of multipath and NLOS could increase if the antenna stays static. As indicated in [33], the speed of the antenna is strongly related to the GNSS positioning error caused by multipath effect.

Pseudorange residue, η: Least square estimation is a basic method to implement the triangulation which is the principle of GPS positioning. With the least squares estimation, the receiver states can be estimated using (1).

$$\hat{\boldsymbol{r}} = (\boldsymbol{G}^T\boldsymbol{G})^{-1}\boldsymbol{G}^T\boldsymbol{\rho} \tag{1}$$

where $\boldsymbol{r}$ is the receiver states, including 3-dimentional position and clock offset between receiver and GPS system time. $\boldsymbol{\rho}$ denotes the pseudorange measurement. $\boldsymbol{G}$ denotes the measurement matrix consisting of the unit LOS vector between the satellite and receiver. The inconsistency between the pseudorange measurements can be expressed by η and calculated as:

$$\hat{\boldsymbol{\eta}} = \boldsymbol{\rho} - \boldsymbol{G}\cdot\boldsymbol{r} \tag{2}$$

As indicated in the previous study [14], the pseudorange residual can be regarded as an indicator to exclude multipath and NLOS signal if the number of measurement is sufficient.

Difference between delta pseudorange and pseudorange rate $|\Delta\rho - \dot{\rho}\cdot\Delta t|$: The idea of this variable to check the consistency between the measurements of pseudorange and Doppler shift. The pseudorange and Doppler shift are estimated by code and frequency/carrier tracking loops, respectively. Namely, they are independent if neglecting their trivial cross-correlation. Delta pseudorange indicates the change of pseudorange between two epochs. It is calculated by:

$$\Delta\rho_k^{(i)} = \rho_k^{(i)} - \rho_{k-1}^{(i)} \tag{3}$$

where superscript *(i)* and subscript *k* denote index of satellite and epoch, respectively. Pseudorange rate $\dot{\rho}$ also indicates the change of pseudorange between two epochs. It can be calculated by Doppler shift based on the principle of Doppler effect as:

$$\dot{\rho}^{(i)} = f_{Doppler}^{(i)} - \frac{c}{f_{L1}} \tag{4}$$

where $f_{Doppler}$ denotes the Doppler shift in unit of Hz, c denotes the speed of light and f_{L1} denotes the GPS L1 band carrier frequency, which is 1575.42 MHz. Thus, their difference can be calculated by $|\Delta\rho - \dot{\rho} \cdot \Delta t|$, where Δt is the time difference between two epochs.

The labelled data with respect to the above listed variable is shown in the figure below. The figure on the top panel clearly shows tne most of the clean LOS data has strong received signal strength comparing to the others. The C/N_0 of multipath is within a wide range between 25 to 40 dB-Hz. The C/N_0 of NLOS is rarely larger than 35 dB-Hz and mainly between 25 to 30 dB-Hz. In terms of change rate of C/N_0, multipath has no distinct feature, it is widely distributed between -20 to 20 dB-Hz. NLOS is distributed between -10 to 10 dB-Hz. With regards to pseudorange residue, LOS has much smaller value because they are consistent to majority of received measurement. It is clear that NLOS distributes more on the positive than negative value. This phenomenon is due to the NLOS travels additional route comparing to LOS. Thus, its pseudorange error tends to be positive value. To observe the bottom column, LOS signal has better consistency between pseudorange and Doppler shift measurements than that of multipath and NLOS. Comparing to multipath and NLOS, they are similar in the range between -10 to 10 meters. However, NLOS has wider range of difference between delta pseudorange and pseudorange rate. This difference will be shown in the next section.

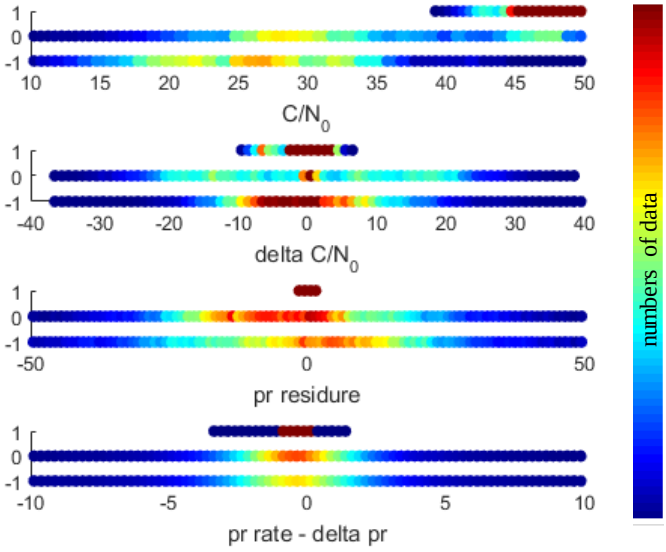

Fig. 5. Labelled LOS, Multipath and NLOS (1, 0 and -1 in Y-axis) data with respected to the GPS variables in X-axis. Color denotes the number of data.

V. SUPPORT VECTOR MACHINE

A. Algorithm and Toolbox

A linear representation of the regressor, classes y and features x is expressed as:

$$y(x) = \mathrm{w}^T\varphi(x), x \in \mathbb{R} \tag{5}$$

where $\varphi(\cdot)$ denotes a manipulatable function that predefined according to application. w denotes the parameter of regressor, which is the parameter estimated by machine learning approach. A SVM is a supervised machine learning technique used for classification. Its regressor can be understood as hyperplanes to separate different classes [34]. The hyperplanes of SVM can be described as:

$$\text{minimize } \|\mathrm{w}\|^2 \text{ s.t. } \begin{matrix} y - \mathrm{w}^T\varphi(x) \le \varepsilon \\ y - \mathrm{w}^T\varphi(x) \ge -\varepsilon \end{matrix} \tag{6}$$

where ε denotes the margin of the hyperplane. If the margin is small (i.e., almost zero), implying the trained classifier cannot clearly separate the classes based on the given features. To obtain the given equation (6), its optimization can be expressed as:

$$\text{minimize } \|\mathrm{w}\|^2 + \gamma \sum_{k=1}^{N} L\left(y_k - \mathrm{w}^T\varphi(x_k)\right) \tag{7}$$

where r denotes regularization parameter, which is used to balance the trade-off between model complexity and training error. Finally, it can be expressed as:

$$y(x) = \sum_{k=1}^{N} \alpha_k \phi(x, x_k) \tag{8}$$

where

$$\phi(x, x_k) = \varphi(x)^T\varphi(x_k) \tag{9}$$

$\phi(\cdot,\cdot)$ denotes a kernel function and α can be estimated using sophisticated toolbox. This paper applies SVM provided by Matlab [35]. This paper uses the default setting of Matlab to quickly demonstrate the effectiveness of SVM to classify clean and biased GNSS pseudorange measurement. In the default setting, the linear kernel, $\phi(x, x_k) = x^T x$ is used. There is other setting could better fit this GNSS LOS, multipath and NLOS classification. This paper uses the default setting of Matlab to quickly demonstrate the effectiveness of SVM to classify clean and biased GNSS pseudorange measurement.

B. Classifaction Result

To avoid the unbalance problem of the training dataset, identical numbers of LOS, multipath, and NLOS measurement are used. There are 85,365 samples used. This sample will be divided into 10 sets to conduct the 10 – fold classification [36]. The classification accuracies using single feature listed in Section IV are compared in TABLE I.

TABLE I. LOS, MULTIPATH AND NLOS CLASSIFICATION ACCURACY USING SINGLE FEATURE.

Received signal strength	Change rate of received signal strength	Pseudorange residue	Difference between delta pseudorange and pseudorange rate
67.1%	39.4%	40.5%	65.4%

As shown in TABLE I, the classification accuracy using the feature of pseudorange residue is less than 50%. In deep urban

canyon, the number of NLOS and multipath could be more than that of LOS in a single epoch data. It results in the pseudorange residue cannot be a distinct feature to classify the types of GNSS received signal. The accuracy using change rate of RSS as feature is less than 40%. The change rate of RSS can successfully separate clean and biased measurement. However, it has no capability to separate multipath and NLOS. The classification results using the rest two features can achieve more than 65%. Fig. 6 and 7 show the labelled data in the perspectives of received signal strength and the difference between delta pseudorange (from pseudorange measurement) and pseudorange rate (from Doppler shift).

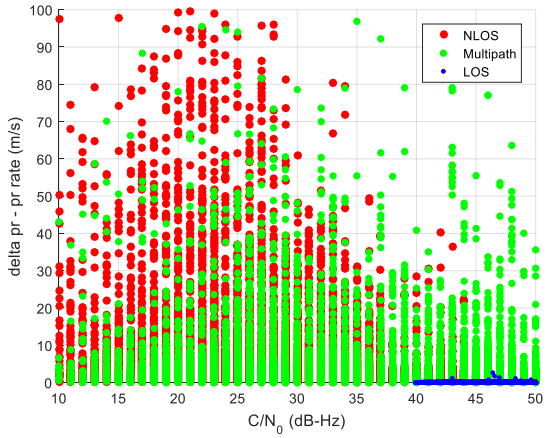

Fig. 6. Labelled data of LOS, multipath and NLOS. X and Y axes are RSS and $|\Delta\rho - \dot{\rho} \cdot \Delta t|$, respectively.

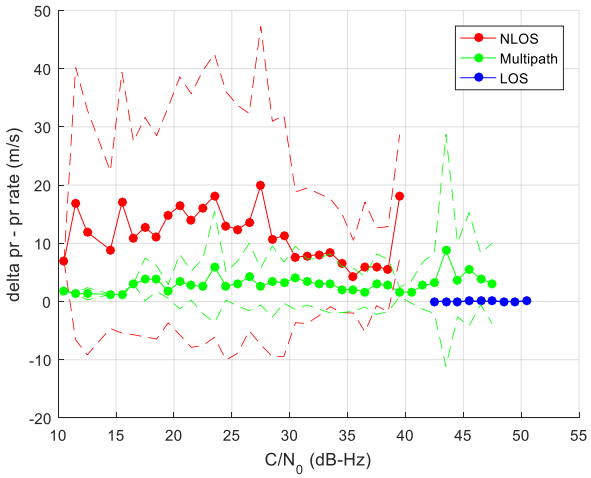

Fig. 7. Mean and standard deviation of $|\Delta\rho - \dot{\rho} \cdot \Delta t|$ in terms of C/N_0. Solid and dash lines denote the mean and mean plus/minus a standard deviation, respectively.

To observe Figs. 6 and 7, it is obvious that LOS, multipath and NLOS can be easily divided into three groups based on these two features. For example, the measurement is very likely to be NLOS if the C/N_0 is larger than 40 dB-Hz and $|\Delta\rho - \dot{\rho} \cdot \Delta t|$ is less than 2 meters. Based on this logic, the SVM classifier trained using multiple features are listed in TABLE II. There are three features are used, 1) RSS, 2) pseudorange residue and 3) difference between delta pseudorange and pseudorange rate. Using both the first and last features, the classification accuracy will achieve about 75%. If all the features mentioned in Section IV are used to train a SVM classifier, then still about 75% of accuracy is achieved. In the other words, it is not improved using additional two features.

TABLE II. LOS, MULTIPATH AND NLOS CLASSIFICATION ACCURACY USING MULTIPLE FEATURES.

Received signal strength Difference between delta pseudorange and pseudorange rate	Received signal strength Pseudorange residue	Pseudorange residue Difference between delta pseudorange and pseudorange rate
75.4%	69.9%	66.8%

VI. CONCLUSIONS AND FUTURE WORK

This paper applies a machine learning approach to distinguish the received GPS signal types, namely LOS, multipath and NLOS, using several features extracted from raw measurements. Four features including 1) received signal strength, 2) change rate of RSS, 3) pseudorange residue and 4) difference between delta pseudorange and pseudorange rate are discussed. According to the experiment result, about 75% of classification accuracy can be achieved using a SVM classifier trained by the first and the last features.

This work is a pilot study to show the effeteness of the machine learning approaches in GNSS positioning. It is important to note the classifier developed can only be applied to static applications. Future work of this study is to train the classifier using dynamic dataset. In addition, different machine learning approaches, such as decision tree, will be applied to find the most reliable classifier.

ACKNOWLEDGEMENT

The author greatly appreciates Mr. Guohao Zhang collecting the static GNSS dataset.

REFERENCES

[1] S. Miura, L. T. Hsu, F. Chen, and S. Kamijo, "GPS Error Correction With Pseudorange Evaluation Using Three-Dimensional Maps," *Intelligent Transportation Systems, IEEE Transactions on*, vol. 16, no. 6, pp. 3104 - 3115, 2015.

[2] Y. Gu, L.-T. Hsu, and S. Kamijo, "GNSS/On-Board Inertial Sensor Integration with the Aid of 3D Building Map for Lane-Level Vehicle Self-Localization in Urban Canyon," *Vehicular Technology, IEEE Transactions on*, vol. 65, no. 6, pp. 4274-4287, 2015.

[3] S. T. S. Thong, C. T. Han, and T. A. Rahman, "Intelligent Fleet Management System with Concurrent GPS & GSM Real-Time Positioning Technology," in *2007 7th International Conference on ITS Telecommunications*, 2007, pp. 1-6.

[4] Q. J. Kong, Q. Zhao, C. Wei, and Y. Liu, "Efficient Traffic State Estimation for Large-Scale Urban Road Networks," *IEEE Transactions on Intelligent Transportation Systems*, vol. 14, no. 1, pp. 398-407, 2013.

[5] M. Ortiz, D. Bétaille, F. Peyret, O. M. Lykkja, and S. P. Oseth, "Assessment of end-to-end performances of a GNSS-based road user charging system based on IFSTTAR-GEOLOC and Q-Free cooperation," in *2016 European Navigation Conference (ENC)*, 2016, pp. 1-8.

[6] R. Sun, W. Y. Ochieng, and S. Feng, "An integrated solution for lane level irregular driving detection on highways," *Transportation Research Part C: Emerging Technologies*, vol. 56, pp. 61-79, 2015/07/01/ 2015.

[7] P. Merdrignac, O. Shagdar, and F. Nashashibi, "Fusion of Perception and V2P Communication Systems for the Safety of Vulnerable Road Users," *IEEE Transactions on Intelligent Transportation Systems*, vol. PP, no. 99, pp. 1-12, 2016.

[8] S. B. Cruz, T. E. Abrudan, Z. Xiao, N. Trigoni, and J. Barros, "Neighbor-Aided Localization in Vehicular Networks," *IEEE Transactions on Intelligent Transportation Systems*, vol. PP, no. 99, pp. 1-10, 2017.

[9] P. D. Groves, *Principles of GNSS, Inertial, and Multi-Sensor Integrated Navigation Systems (GNSS Technology and Applications)*, 2nd ed. Artech House Publishers, 2013.

[10] V. A. Veitsel, A. V. Zhdanov, and M. I. Zhodzishsky, "The Mitigation of Multipath Errors by Strobe Correlators in GPS/GLONASS Receivers," (in English), *GPS Solutions*, vol. 2, no. 2, pp. 38-45, 1998/10/01 1998.

[11] J. J. Spilker, "Fundamentals of Signal Tracking Theory," in *Global Positioning System: Theory and Application*, vol. 1, B. W. Parkinson, Ed. Washington DC: American Institute of Aeronautics, 1996.

[12] Z. Jiang and P. Groves, "NLOS GPS signal detection using a dual-polarisation antenna," (in English), *GPS Solutions*, vol. 18, no. 1, pp. 15-26, 2014/01/01 2014.

[13] L.-T. Hsu, S.-S. Jan, P. Groves, and N. Kubo, "Multipath mitigation and NLOS detection using vector tracking in urban environments," (in English), *GPS Solutions*, vol. 19, no. 2, pp. 249-262, April 2015.

[14] L. T. Hsu, H. Tokura, N. Kubo, Y. Gu, and S. Kamijo, "Multiple Faulty GNSS Measurement Exclusion Based on Consistency Check in Urban Canyons," *IEEE Sensors Journal*, vol. 17, no. 6, pp. 1909-1917, 2017.

[15] K.-W. Chiang, T. Duong, and J.-K. Liao, "The Performance Analysis of a Real-Time Integrated INS/GPS Vehicle Navigation System with Abnormal GPS Measurement Elimination," *Sensors*, vol. 13, no. 8, pp. 10599-10622, 2013.

[16] W. Gurtner, "INNOVATION: RINEX--THE RECEIVER INDEPENDENT EXCHANGE FORMAT," *GPS world*, vol. 5, no. 7, pp. 48-53, 1994.

[17] Google. (2016). *Android API: GnssMeasurement*. Available: https://developer.android.com/reference/android/location/GnssMeasurement.html

[18] P. D. Groves, "Shadow Matching: A New GNSS Positioning Technique for Urban Canyons," *The Journal of Navigation*, vol. 64, no. 03, pp. 417-430, 2011.

[19] L. Wang, P. D. Groves, and M. K. Ziebart. (2013) Urban positioning on a smartphone: Real-time shadow matching using GNSS and 3D city models. *Inside GNSS*. 44-56.

[20] D. Betaille, F. Peyret, M. Ortiz, S. Miquel, and L. Fontenay, "A New Modeling Based on Urban Trenches to Improve GNSS Positioning Quality of Service in Cities," *Intelligent Transportation Systems Magazine, IEEE*, vol. 5, no. 3, pp. 59-70, 2013.

[21] S. Peyraud *et al.*, "About Non-Line-Of-Sight Satellite Detection and Exclusion in a 3D Map-Aided Localization Algorithm," *Sensors*, vol. 13, no. 1, pp. 829-847, 2013.

[22] F. Peyret, D. Bétaille, P. Carolina, R. Toledo-Moreo, A. F. Gómez-Skarmeta, and M. Ortiz, "GNSS Autonomous Localization: NLOS Satellite Detection Based on 3-D Maps," *IEEE Robotics & Automation Magazine*, vol. 21, no. 1, pp. 57-63, 2014.

[23] T. Suzuki and N. Kubo, "Correcting GNSS Multipath Errors Using a 3D Surface Model and Particle Filter," in *Proceedings of the 26th International Technical Meeting of The Satellite Division of the Institute of Navigation (ION GNSS+ 2013)*, Nashville, TN, 2013, pp. 1583-1595.

[24] L.-T. Hsu, F. Chen, and S. Kamijo, "Evaluation of Multi-GNSSs and GPS with 3D Map Methods for Pedestrian Positioning in an Urban Canyon Environment," *IEICE Transactions on Communications and Computer Sciences, Special Issue on Intelligent Transportation System*, vol. E98-A, no. 1, January 2015 2015.

[25] L.-T. Hsu, Y. Gu, Y. Huang, and S. Kamijo, "Urban Pedestrian Navigation using Smartphone-based Dead Reckoning and 3D Maps Aided GNSS," *Sensors Journal, IEEE*, vol. 16, no. 5, pp. 1281-1293, 2016.

[26] N. M. Drawil, H. M. Amar, and O. A. Basir, "GPS Localization Accuracy Classification: A Context-Based Approach," *IEEE Transactions on Intelligent Transportation Systems*, vol. 14, no. 1, pp. 262-273, 2013.

[27] H.-S. Wang, C.-Y. Kao, and J.-F. Chen, "Sequential Quadratic Method for GPS NLOS Positioning in Urban Canyon Environments," *International Journal of Automation and Smart Technology*, Non-Line-of-Sight; Sequential Quadratic Programming; Global Positioning System; Wilcoxon Regression; Urban Canyon Environment. vol. 3, no. 1, pp. 37-46, 2013.

[28] Q.-H. Phan, S.-L. Tan, and I. McLoughlin, "GPS multipath mitigation: a nonlinear regression approach," *GPS Solutions*, journal article vol. 17, no. 3, pp. 371-380, 2013.

[29] N. Sokhandan, A. Broumandan, and G. Lachapelle, "GNSS Multipath Mitigation using Low Complexity Adaptive Equalization Algorithms," in *5th International Colloquium Scientific and Fundamental Aspects of the Galileo Programme* Braunschweig, Germany, 2015.

[30] M. Socharoentum and H. A. Karimi, "A Machine Learning Approach to Detect Non-Line of Sight Satellites in Nav2Nav," in *23rd ITS World Congress*, Melbourne, Australia, 2016.

[31] R. Yozevitch, B. B. Moshe, and A. Weissman, "A Robust GNSS LOS/NLOS Signal Classifier," *Navigation*, vol. 63, no. 4, pp. 429-442, 2016.

[32] L. Lau and P. Cross, "Development and testing of a new ray-tracing approach to GNSS carrier-phase multipath modelling," (in English), *Journal of Geodesy*, vol. 81, no. 11, pp. 713-732, 2007/11/01 2007.

[33] N. Kubo, R. Kikuchi, and M. Higuchi, "A Unique Approach to Strong Multipath Mitigation in Dense Urban Areas," in *Proceedings of ION GNSS+ 2015*, Tampa, Florida, 2015, pp. 2905-2913.

[34] H. Wymeersch, S. Marano, W. M. Gifford, and M. Z. Win, "A Machine Learning Approach to Ranging Error Mitigation for UWB Localization," *IEEE Transactions on Communications*, vol. 60, no. 6, pp. 1719-1728, 2012.

[35] S. Canu, Y. Grandvalet, V. Guigue, and A. Rakotomamonjy, "Svm and kernel methods matlab toolbox," *Perception Systmes et Information, INSA de Rouen, Rouen, France*, vol. 2, no. 21, 2005.

[36] C. E. Rasmussen, "Gaussian processes for machine learning," 2006.